

Dipolar Stabilization of Emissive Singlet Charge Transfer Excited States in Polyfluorene Copolymers

Fernando B. Dias,^{*,†} Simon King,[†] Andrew P. Monkman,[†] Irene I. Perepichka,^{‡,||} Maxim A. Kryuchkov,^{‡,||} Igor F. Perepichka,^{*,‡,§} and Martin R. Bryce[‡]

OEM Research Group, Department of Physics, Durham University, Durham DH1 3LE, U.K., Department of Chemistry, Durham University, Durham DH1 3LE, U.K., and Centre for Materials Science, Faculty of Science and Technology, University of Central Lancashire, Preston PR1 2HE, U.K.

Received: January 4, 2008; Revised Manuscript Received: March 10, 2008

The singlet excited-state dynamics in poly[(9,9-dioctylfluorene)–(dibenzothiophene-*S,S*-dioxide)] (PFS_x) random copolymers with different contents of dibenzothiophene-*S,S*-dioxide (S) units have been studied by steady-state and time resolved fluorescence spectroscopies. Emission from PFS_x copolymers shows a pronounced solvatochromism in polar chloroform, relative to the less polar toluene. An excited intramolecular charge transfer state (ICT) is stabilized by dipole–dipole interactions with the polar solvent cage, and possibly accompanied by conformational rearrangement of the molecular structure, in complete analogy with their small oligomer counterparts. The spectral dynamics clearly show that the ICT stabilization is strongly affected by the surrounding medium. In the solid state, emission from PFS_x copolymers depends on the content of S units, showing an increase of inhomogeneous broadening and a red shift of the optical transitions. This observation is consistent with stabilization of the emissive ICT state, by the local reorientation of the surrounding molecules at the location of the excited chromophore, which results in favorable dipole–dipole interactions driven by the increase in the dielectric constant of the bulk polymer matrix with increasing S content, in analogy to what happens in polar solvent studies. Furthermore, in clear agreement with the interpretation described above, a strong increase in the emission quantum efficiency is observed in the solid state by decreasing the temperature and freezing out the molecular torsions and dipole–dipole interactions necessary to stabilize the ICT state.

1. Introduction

Semiconductive organic conjugated polymers (CPs) have been the focus of intense research during the past two decades due to their potential in plastic electronics, e.g., as active components in polymer-based light-emitting devices (PLEDs).^{1–5} Optimization of organic PLEDs for various applications aims for high efficiencies and more reliable devices, with an emphasis on trying to improve both the tuning of the emission and the stability across the entire visible spectrum, together with a better balance on the charge injection. One way to achieve this goal is through copolymerization, i.e., chemically modifying the emissive polymer,^{3,6} in order to match the energy levels of the copolymer's highest occupied and lowest unoccupied molecular orbitals, HOMO and LUMO, respectively, with the work functions of the electrodes.

Copolymerization, however, frequently leads to materials with different photophysical properties, which can be affected by, for example, the relative order of the comonomers' energy levels, polymer concentration, or even medium polarity. Systematic studies on the effect of incorporating different monomer units into CPs are, therefore, crucial to achieving a good understanding of fundamental aspects of the physics involved,

as well as providing guidelines in order to develop new strategies for practical applications.

Among the large class of CPs, fluorene-based polymers and copolymers are currently the most promising for electroluminescent applications due to their normally strong blue emission and excellent thermal, chemical, and electrochemical stabilities.^{3,5}

Recently we have reported the synthesis and photophysical characterization of fluorene–dibenzothiophene-*S,S*-dioxide co-oligomers.^{7,8} These co-oligomers show improved electron affinity and stability with regard to both p- and n-doping and retain high photoluminescence efficiencies in solution and the solid state.⁷ Furthermore, these co-oligomers have shown a strong solvatochromism of their emission with increasing solvent polarity.⁸ In nonpolar solvents the emission appears narrow with well-resolved features, suggesting the presence of a local excited state (LE) that is associated with the electron density being distributed along the fluorene conjugated backbone, analogous to fluorene based polymer counterparts. However, in polar solvents, only a featureless broad emission is observed at longer wavelengths, which indicates the presence of an intramolecular excited charge transfer state (ICT), stabilized by the reorganization of the polar solvent and possibly accompanied by large-amplitude molecular motions of the excited solute molecule.⁸

The present study expands the work done with co-oligomers to analogous fluorene copolymers with different fractions of dibenzothiophene-*S,S*-dioxide (S) units randomly distributed along the polymer backbone (poly[(9,9-dioctylfluorene)–(dibenzothiophene-*S,S*-dioxide)], PFS_x). We demonstrate that the formation of an ICT state in polar medium is stabilized by the reorientation of

* To whom correspondence should be addressed. Telephone: +44-(0)191-334-3590 (F.B.D.); +44-(0)1772-89-3758 (I.F.P.). E-mail: f.m.b.dias@durham.ac.uk (F.B.D.); iperepichka@uclan.ac.uk (I.F.P.).

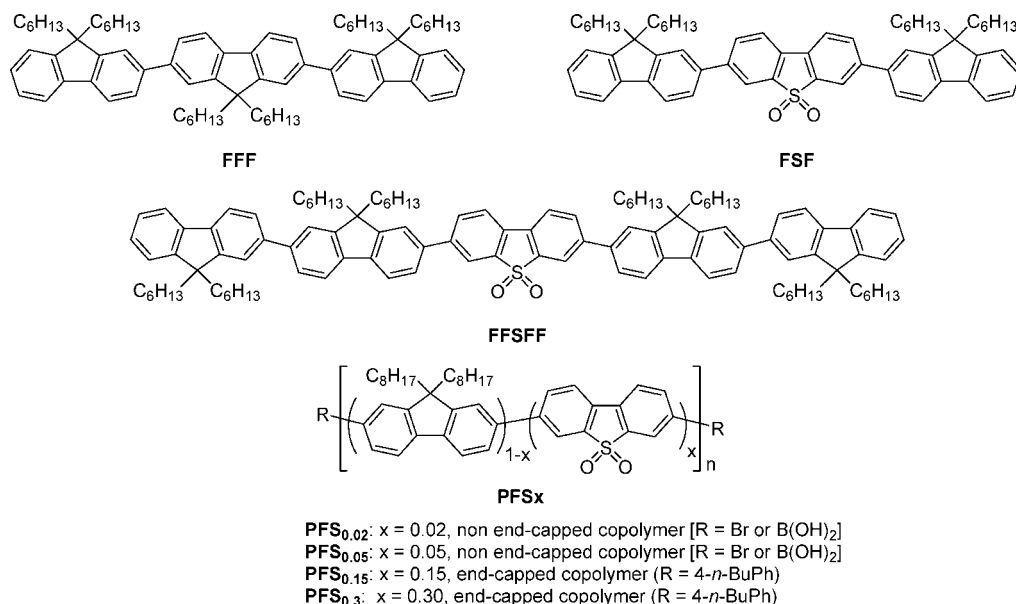
[†] Department of Physics, Durham University.

[‡] Department of Chemistry, Durham University.

[§] University of Central Lancashire.

^{||} Current address: Department of Chemistry, University of Montreal, Montreal, Québec, H3C 5G4, Canada.

CHART 1: Chemical Structures of the Compounds Studied



the polar solvent cage at the location of the excited solute, in a direct analogy to what happens in the short oligomers.

The spectral dynamics of the PFS_x copolymers have also been studied in the solid state, and evidence has been obtained for the stabilization of the ICT state by reorientation of the surrounding molecules at the excited solute location, due to dipole–dipole interactions between the excited solute and the bulk polymer matrix.

Relative to a trimer of 9,9-dihexylfluorene (FFF) (ground-state dipole moment $\mu_G = 0.17$ D, from DFT B3LYP/6-31G(d) calculations in the gas phase; see Table S1 in Supporting Information), the 3,7-bis(9,9-dihexylfluorene-2-yl)dibenzothioophene-*S,S*-dioxide (FSF) co-oligomer ($\mu_G = 5.7$ D) is already a polar molecule in the ground state⁸ and increasing the content of the dibenzothioophene-*S,S*-dioxide (S) units in the copolymer chain leads to an increase of the dielectric constant of the bulk polymer matrix with impact on the photoluminescence (PL) from thin solid films of PFS_x copolymers.

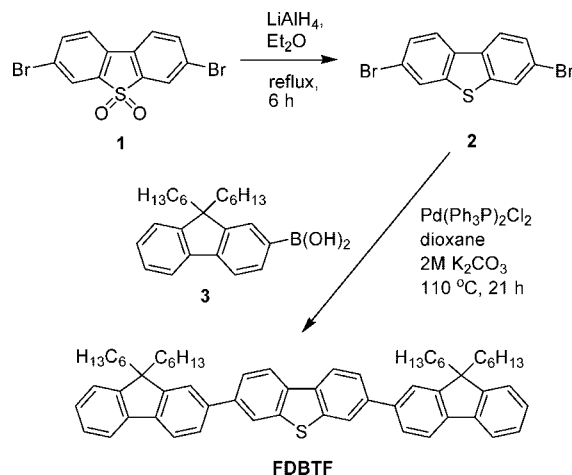
2. Results and Discussion

2.1. Synthesis. The synthesis of the co-oligomers FSF and FFSFF (see Chart 1 for structures) has been described previously.⁷ The synthesis of copolymers PFS_x [$x = 0.02, 0.05, 0.15$, and 0.3 , corresponding to the molar fraction of S units in a random (9,9-dioctylfluorene)–(dibenzothioophene-*S,S*-dioxide) copolymer] will be published elsewhere.⁹

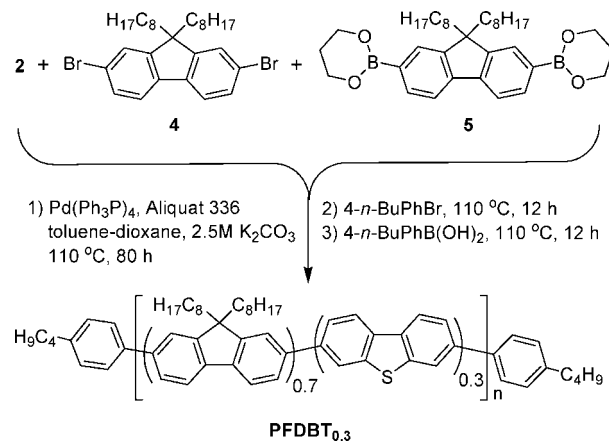
3,7-Dibromothiophene-*S,S*-dioxide (**1**)⁷ was reduced by lithium aluminum hydride in diethyl ether, similar to the procedure described previously,¹⁰ to yield 3,7-dibromodibenzothiophene (**2**). Pd-catalyzed condensation of dibromide **2** with 9,9-dihexylfluorene-2-boronic acid (**3**)⁷ in dioxane/2 M aqueous K₂CO₃ at reflux for 21 h resulted in co-oligomer FDBTF in near-quantitative yield (Scheme 1).

Random (9,9-dioctylfluorene)–(dibenzothiophene) copolymer with 0.3 molar fraction of dibenzothiophene units, PFDBT_{0.3}, was obtained by Suzuki coupling of dibromides **2** and **4** with diboronic ester **5** with the molar ratio of monomers 0.3:0.2:0.5 (Scheme 2). The synthesis was performed in toluene–dioxane–2.5 M aqueous K₂CO₃ mixture with Aliquat 336 as phase transfer reagent and Pd(Ph₃P)₄ as catalyst at 110 °C for 80 h. The resulting copolymer was then end-capped with 4-*n*-

SCHEME 1: Synthesis of FDBTF Co-oligomer



SCHEME 2: Synthesis of PFDBT_{0.3} Copolymer



butylphenyl groups by adding subsequently 4-*n*-butylbromobenzene and 4-*n*-butylphenylboronic acid and heating at 110 °C for 12 h in each case. After purification procedures (by extraction and reprecipitation), high molecular weight copolymer PFDBT_{0.3} ($M_w = 56\,500$ Da, $M_w/M_n = 2.44$) was obtained in 88% yield. The copolymer showed good thermal stability with $T_d^{5\%} = 397$ °C, typical for polyfluorenes.

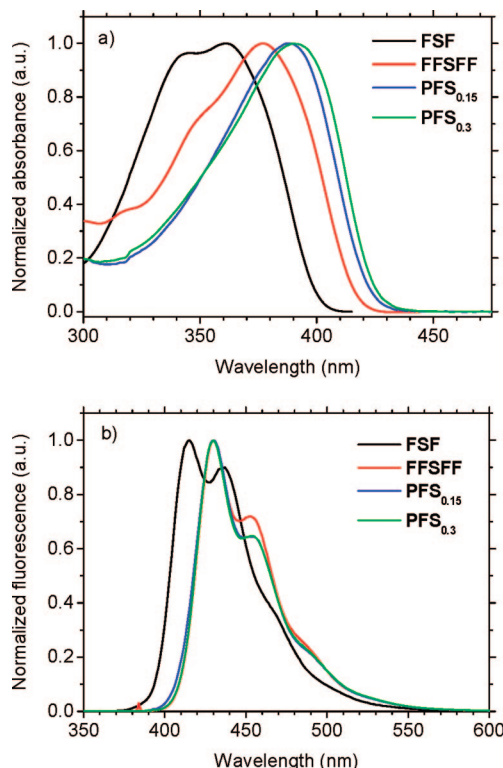


Figure 1. Normalized (a) absorption and (b) emission spectra of FSF, FFSFF, PFS_{0.15}, and PFS_{0.3} in dilute toluene solution. Excitation at 390 nm.

2.2. Solution Optical Properties. 2.2.1. Absorption and Emission Spectra in Dilute Toluene Solution. The absorption spectra of FSF, FFSFF, PFS_{0.15}, and PFS_{0.3} in toluene solution are shown in Figure 1a. A consistent red shift is observed on going from the smaller oligomer FSF to the copolymers PFS_x, denoting the presence of relatively longer conjugated segments in the two copolymers. Figure 1b shows the fluorescence emission spectra of the same four compounds in toluene solution; again a red shift is observed in emission, with the two copolymers emitting at longer wavelengths. Note that no significant alterations are observed in the spectral profile between oligomers and copolymers, and that the emission of the longer oligomer, FFSFF, already matches well the emission of the random copolymers with a relatively high content of S units, showing a larger Stokes shift. Similar spectra were obtained for copolymers with 2 and 5 mol % content of S units, PFS_{0.02} and PFS_{0.05}.

2.2.2. Solvatochromism of PFS_x Copolymers. As a consequence of a photoinduced charge transfer occurring in the FSF and FFSFF excited states,⁸ the emission spectral profile of these relatively small oligomers shows important changes in polar solvents (see Figure S1 in Supporting Information). The intramolecular charge transfer excited state (ICT) is stabilized by increasing the solvent polarity, due to the reorientation of the solvent molecules that are surrounding the excited solute and leading to favorable dipole–dipole interactions;¹¹ further molecular structural arrangements of the solute itself are also possibly involved.¹² In nonpolar solvents the emission is very similar to polyfluorenes, but in polar medium a broad and unresolved emission is observed independent of the excitation wavelength.

Figure 2a shows the absorption and emission spectra of PFS_{0.3} in toluene and in chloroform, a moderately polar solvent. As was observed for FSF and FFSFF,⁸ the absorption spectra of

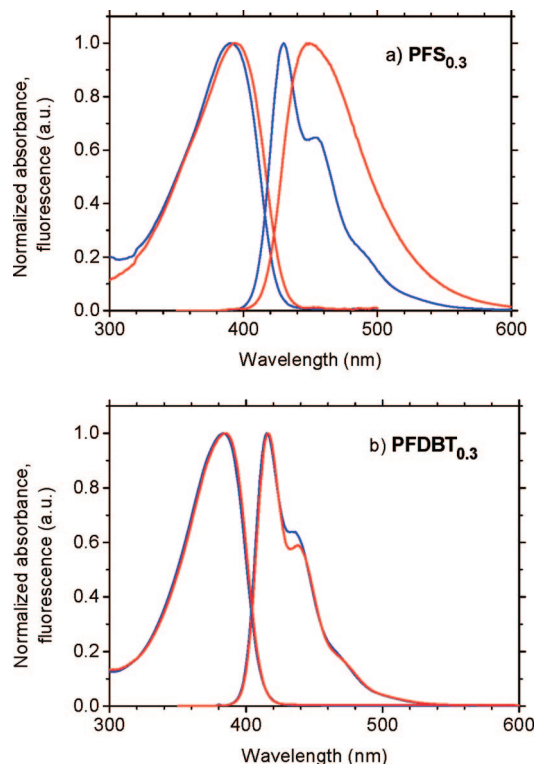


Figure 2. Normalized absorption and emission spectra of (a) PFS_{0.3} and (b) PFDBT_{0.3} in toluene (blue) and chloroform (red). Excitation at 390 nm.

PFS_{0.3} demonstrate relatively small changes with solvent polarity. However, the changes in the emission spectral profile are more pronounced. In toluene the emission maximum is blue-shifted and the spectrum shows the typical vibronic structure observed in fluorene-based polymers,^{3,5} whereas in chloroform, only a broad unresolved emission spectrum is observed, as a consequence of solvent-induced stabilization of the ICT state.

In contrast to that, both absorption and emission spectra of random copolymer PFDBT_{0.3} do not show such drastic changes when comparing toluene to chloroform solutions (Figure 2b). In this copolymer, the charge transfer does not occur due to the lower electron affinity of dibenzothiophene (DBT) units compared to S units, and in both solvents a “polyfluorene-like” emission spectral profile is observed.

Similar to that, a comparison of the absorption spectra of FSF and FDBTF co-oligomers in methanol solution shows a clear red-shifted absorption band for FSF relative to the FDBTF spectrum (see Figure S2 in Supporting Information). A perfect overlap between the blue edges of the two absorption spectra is observed, suggesting that the FSF spectrum is in fact a composition of two different absorptions. One, occurring around 340 nm and overlapping the FDBTF absorption spectrum, corresponds to delocalization of the electron density along the conjugation chain, as in “normal” fluorene homopolymers and oligomers. Another one, at slightly lower energies, is red-shifted and decreased in intensity with increasing solvent polarity,⁸ and is attributed to a state with CT character where the electron density is localized on the central S unit (see Figure S3 in Supporting Information for a representation of the HOMO and LUMO energy levels of FSF and FDBTF oligomers).

The HOMO–LUMO energy levels of the pentamer of 9,9-dihexylfluorene (FFFFF) relative to that of FFSFF⁷ (see Figure S3 in Supporting Information) clearly show that S moieties act as energy traps in the copolymer chain. Despite the small overlap

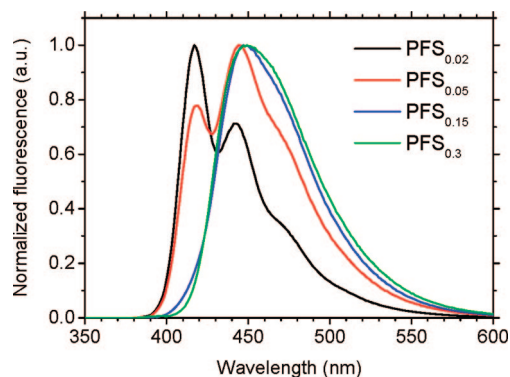


Figure 3. Normalized emission spectra of PFS_x copolymers with increasing percentage of S units in chloroform solution. Note the dual fluorescence observed even at small percentage of S units (5 mol %). Excitation at 390 nm.

between the FFSFF absorption and the polyfluorene emission [poly(9,9-dioctylfluorene), PFO] (see Figure S4 in Supporting Information), the extinction coefficient of FFSFF co-oligomer is large (molar extinction coefficient $\epsilon_\lambda \sim 115\,000 \text{ L mol}^{-1} \text{ cm}^{-1}$ at 380 nm), and Förster energy transfer from polyfluorene-like regions to FFSFF moieties in solution and in the solid state will be operative and quite efficient ($R_0 \sim 36 \text{ \AA}$). As a consequence, the fluorescence of the random copolymers PFS_x would be strongly affected by the presence of S units. However, since the stabilization of the ICT state is dependent on the local bulk polarity at the solute location, either a polyfluorene-like or a broad unresolved and red-shifted emission would be observed in nonpolar medium and polar medium, respectively.

Figure 3 shows the emission spectra of PFS_x copolymers with different contents of S units randomly distributed along the polymer backbone (2, 5, 15, and 30 mol %), in dilute chloroform solution. Chloroform is a relatively polar solvent (dielectric permittivity $\epsilon \sim 4.89$), in which FFSFF moieties show the broad emission characteristic of the ICT stabilization. However, energy migration along an isolated conjugated polymer chain is known to be less efficient than in the solid state,¹³ where interchain pathways are also available, and radiative decay from conjugated fluorene moieties (FFFFF) is able to compete, giving rise to a dual emission profile at lower S percentages.

The evolution of the spectral profile when going from low to high S content clearly agrees with the above interpretation. At low percentages (2 mol %) of S units, the emission mainly occurs from polyfluorene moieties and the relative contribution of emission from FFSFF regions is small. At intermediate content of S units (5 mol %), the spectrum represents a dual emission process, with a polyfluorene-like emission at shorter wavelengths and a broad nonstructured red-shifted FFSFF-like emission. Finally, at higher S content (15 and 30 mol %), the FFSFF-like emission is dominant, and only a small shoulder that indicates emission from polyfluorene-like moieties is observed on the blue side of the spectrum at 15 mol % (Figure 3).

2.2.3. Time Resolved Fluorescence Decays. Time resolved fluorescence decays of FSF and FFSFF co-oligomers and PFDBT_{0.3} and PFS_x copolymers were collected at 293 K in toluene and chloroform solutions, with excitation at 380 nm and emission collected at different wavelengths. Results, decay times, amplitudes, and χ^2 values are shown in Table 1.

Fluorescence decays of polyfluorene derivatives generally show a complex behavior.¹⁴ Excellent fits are frequently only obtained when sums of three discrete exponential functions with components around 30, 100, and 370 ps are used in low-

viscosity solvents. The relative contribution of the intermediate component is usually only residual and decreasing in importance at larger emission wavelengths; the faster component appears at shorter wavelengths as a decay time (positive amplitude) and at longer wavelengths as a rise time (negative amplitude). These two faster components can be assigned to isoenergetic excitation energy transfer¹³ and conformational rearrangements of PF's backbone¹⁴ as a result of thermal fluctuations (see Figure S5 in Supporting Information for results of $\text{PFS}_{0.3}$ decay analysis in toluene with two and three exponential terms).

However, despite this complex pattern, some well-defined trends can be extracted from Table 1. First, note that the emission decay of PFDBT_{0.3} acquired at the maximum emission wavelength (417 nm) in toluene and chloroform is almost completely described by a single-exponential decay with 370 and 390 ps, respectively. Usually, a minor decay component around 30 ps is also observed, but no significant changes with solvent polarity were detected.

Second, the longer decay component in toluene increases from FFSFF to FSF. Similar behavior has been observed previously in fluorene oligomers with lifetimes increasing with decreasing conjugation length.¹⁵ For PFS_x copolymers, the same correlation with increasing S content suggests a decrease in the segment conjugation length imposed by the insertion of S moieties.

Third, the emission decays of PFS_x copolymers in toluene are similar to the emission decay of PFDBT_{0.3}, and agree well with those usually observed in other polyfluorene derivatives.

Finally, both FSF and FFSFF oligomers and PFS_x copolymers in chloroform show a longer component that ranges between 1.47 ns and 850 ps. This component is clearly in agreement with the observations from steady-state data that indicate the stabilization of an ICT state emitting around 450 nm. In fact, at low S content (where dual fluorescence is observed), the relative importance of this component is minor at shorter wavelengths, where the polyfluorene-like emission is predominant, and increases at longer wavelengths, where the broad nonstructured emission is observed. At higher S contents, the signature of the PF-like emission decay is not detected. This is in agreement with no detection of PF-like emission in copolymers with S percentages higher than 5 mol %. However, it is still possible that some mixture of the PF-like and ICT decay components is occurring at shorter wavelengths, explaining the apparent shortening of the ICT lifetime in the blue region of the emission spectrum.

Figure 4 shows the time dependence of $\text{PFS}_{0.3}$ emission in (a) toluene with emission collected at 410 and 500 nm, and (b) chloroform with emission collected at 420 and 550 nm. Note the fast decay observed at the blue side of the emission spectra and the corresponding build in at longer wavelengths. The fastest decay component is clearly more important in chloroform than in toluene, and the emission decays more slowly in the more polar solvent, revealing the presence of a longer-lived species.

Surprisingly, the fast decay component appears with similar magnitude in both toluene and chloroform, around 10 ps, while being far more important in the polar solvent, suggesting that, in our temporal window, the observed spectral dynamics are being controlled by the excited solute molecular relaxation, and that the contribution of the bulk solvent relaxation has occurred in a faster time scale. Further studies involving the characterization of conformationally restricted oligomers are needed in order to disentangle the contribution of the bulk solvent reorientation from the solute structural rearrangements.

2.2.4. Time Resolved Emission Spectra (TRES). Time resolved emission spectra of $\text{PFS}_{0.3}$ in toluene and chloroform

TABLE 1: Values of τ_i , A_i , and χ^2 from Time Resolved Fluorescence Decays of FSF, FFSFF, PFDBT_{0.3}, and PFS_x Copolymers in Toluene and Chloroform Solutions at 293 K

compound	solvent	λ_{em} (nm)	τ_4 (ns):[A_4]	τ_3 (ns):[A_3]	τ_2 (ns):[A_2]	τ_1 (ns):[A_1]	χ^2
FSF	toluene	415	0.03 :[−0.05]		1.08 :[1]		1.12
	CHCl ₃	432	0.01 :[0.06]			1.47 :[0.94]	1.09
FFSFF	toluene	430	0.02 :[−0.08]		0.75 :[1]		1.07
	CHCl ₃	450	0.03 :[0.08]			1.11 :[0.92]	1.09
PFDBT _{0.3}	toluene	417	0.03 :[0.1]		0.37 :[0.9]		1.04
	CHCl ₃	417	0.04 :[0.1]		0.39 :[0.9]		1.02
PFS _{0.02}	toluene	417		0.13 :[0.18]	0.4 :[0.82]		1.04
	CHCl ₃	417		0.12 :[0.22]	0.4 :[0.77]	0.96 :[0.01]	1.1
PFS _{0.05}	toluene	450		0.12 :[0.12]	0.4 :[0.68]	0.96 :[0.2]	1.05
	CHCl ₃	417	0.01 :[0.32]	0.1 :[0.21]	0.41 :[0.45]	0.91 :[0.02]	1.08
PFS _{0.15}	toluene	430	0.01 :[0.1]	0.1 :[0.13]	0.41 :[0.29]	0.91 :[0.48]	1.00
	CHCl ₃	430	0.01 :[0.65]	0.1 :[0.04]	0.55 :[0.96]		1.05
PFS _{0.3}	toluene	430	0.01 :[0.26]	0.1 :[0.08]		0.87 :[0.25]	1.08
	CHCl ₃	410	0.01 :[0.58]	0.082 :[0.1]	0.533 :[0.32]	0.87 :[0.66]	1.08
PFS _{0.3}	CHCl ₃	420	0.013 :[0.18]	0.084 :[0.12]	0.537 :[0.7]		1.07
		450		0.12 :[0.03]	0.543 :[0.97]		1.06
		500	0.015 :[−0.12]		0.55 :[1.00]		1.11
		420	0.012 :[0.77]	0.11 :[0.08]		0.85 :[0.15]	1.13
		430	0.013 :[0.62]	0.13 :[0.09]		0.88 :[0.29]	1.11
		450	0.008 :[0.49]	0.12 :[0.09]		0.91 :[0.51]	1.2
		500	0.015 :[−0.1]	0.16 :[0.07]		0.98 :[0.93]	1.11
		530	0.013 :[−0.21]			1.00 :[1.00]	1.09
		550	0.015 :[−0.28]			1.05 :[1.00]	1.16

solutions were collected using excitation at 380 nm. Figure 5 shows the TRES in toluene and chloroform at different time delays, normalized to one independent of the emission wavelength.

In the nonpolar solvent (toluene), the usual spectral dynamics of PF-like emission are observed, showing in the blue region

of the spectrum a small decrease in the emission intensity with time. The build in observed for the fluorescence intensity collected at longer wavelengths is not detected using the streak camera, which can result from the relatively low importance of

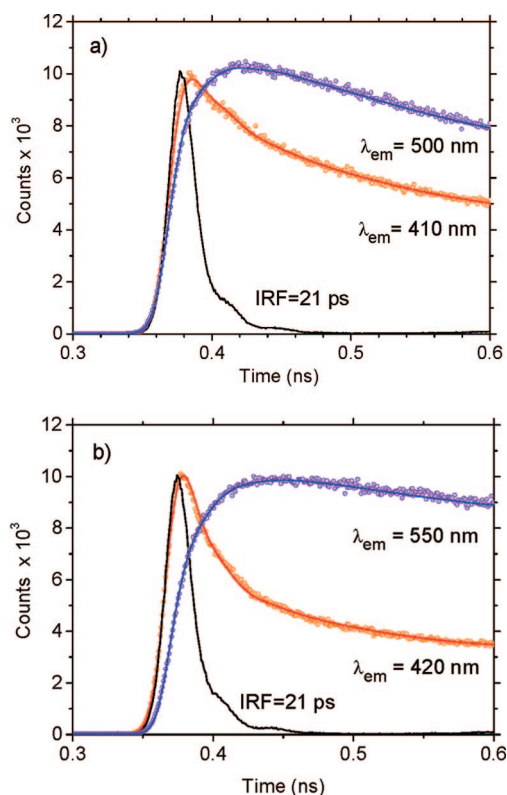


Figure 4. Time resolved fluorescence decay of PFS_{0.3} in (a) toluene, emission collected at 410 and 500 nm, and (b) chloroform, emission collected at 420 and 550 nm. Note the more pronounced spectral dynamics in chloroform when compared with the decay in toluene (see Table 1 for decay components and χ^2 values).

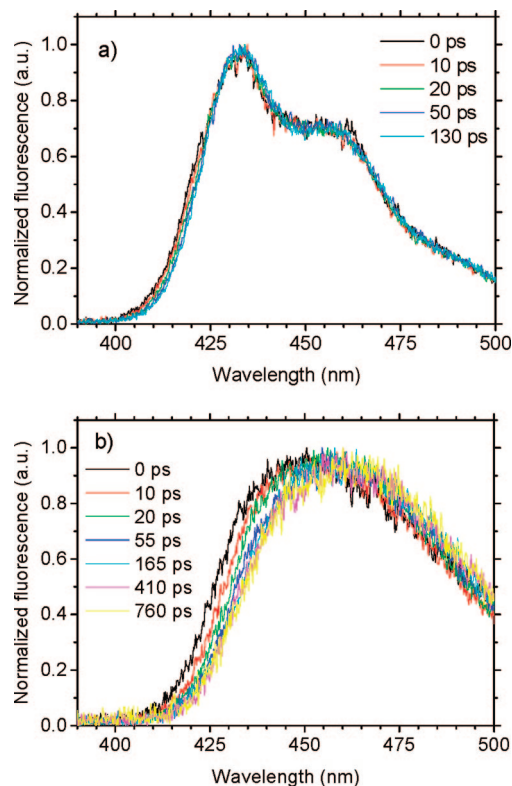
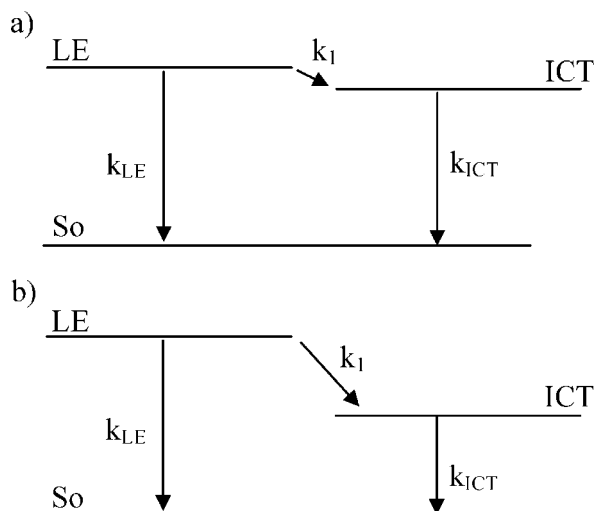


Figure 5. Time resolved emission spectra (TRES) of PFS_{0.3} in (a) toluene and (b) chloroform, normalized independently of the emission wavelength. Excitation at 380 nm. Note that even at time zero no PF-like emission is observed in chloroform. In this (more polar) solvent, pronounced spectral dynamics are revealed showing an emission decrease on the blue side of the spectrum and a build in at longer wavelengths.

SCHEME 3: Schematic Representation of the States Involved in the Excited-State Dynamics of PFS_x Copolymers: (a) Nonpolar Medium and (b) Polar Medium^a



^a k_{LE} , k_I , and k_{ICT} are respectively the rate constants for the LE decay, ICT stabilization, and ICT decay. Increasing the solvent polarity stabilizes the ICT state and emission appears at lower energies.

such a component and the lower signal-to-noise ratio of this system. However, the relatively low importance of such spectral changes is in excellent agreement with the small amplitude of the two faster decay components observed in toluene (Table 1).

In chloroform pronounced spectral dynamics are clearly present: a marked decrease and a build in of the emission intensity are observed over time, at shorter and longer wavelengths, respectively. However, as in the small oligomers, PF-like emission is not observed, even initially, suggesting that the reorientation of the solvent molecules at the location of the excited solute, or at least a part of it, in order to stabilize the ICT state by dipole–dipole interactions, has already occurred below our temporal resolution.

Scheme 3 is a representation of the states involved in the singlet excited state dynamics of PFS_x copolymers, showing the effect of solvent polarity on the stabilization of the ICT state. For historical reasons and to keep the nomenclature used for small oligomers, LE is used to identify the state responsible for the PF-like emission; increasing the medium polarity stabilizes the ICT state and shifts the emission to lower energies.

2.3. Solid-State Optical Properties. 2.3.1. Absorption and Emission Spectra in Solid Thin Films. Studies carried out in very dilute solutions probe essentially intramolecular excitations. However, it has become evident that optical properties of conjugated polymers are also affected by intermolecular interactions that are predominant in the solid state, and consequently optical data collected from solid thin films are more likely to reflect the excitation dynamics present in electroluminescent devices.

In the case of PFS_x copolymers and F/S oligomers, no significant changes, except a slight red shift, were observed in the absorption spectra of solid thin films. As in solution, the absorption is characterized by a broad band that ranges from 300 to 450 nm, showing that no additional states are created by intermolecular interactions. However, the emission spectra of PFS_x copolymers in the solid state no longer present the dual fluorescence nature observed in solution (Figure 6). Now, only one emission band is observed, which is compatible with the

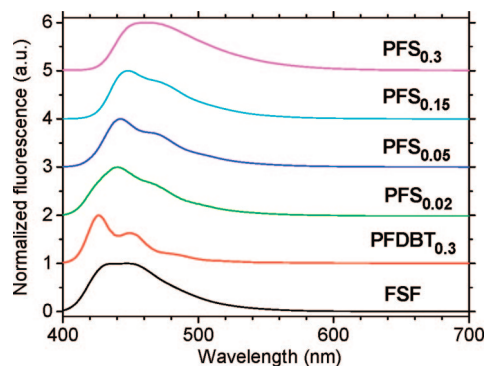


Figure 6. Normalized fluorescence emission spectra of studied compounds spin-coated from toluene solution as thin films on quartz substrates. From bottom: FSF (11 mg/mL), PFDBT_{0.3} (11 mg/mL), PFS_{0.02} (9 mg/mL), PFS_{0.05} (11.2 mg/mL), PFS_{0.15} (9.6 mg/mL), and PFS_{0.3} (8.3 mg/mL). Excitation at 390 nm.

highly efficient energy migration to FFSFF sites in the solid state, making the lowest energy level attainable by almost every excitation.^{13,16}

Interestingly, the emission spectra are still dependent on the sample S content. For high S percentages, the emission appears structureless, as it is in a polar medium, but when the S content is low or absent (as in the case of PFDBT_{0.3}), the emission is structured, as it is in a nonpolar environment. Note that the low content of S units cannot explain by itself the absence of a broad unstructured emission. For example, for PFS_{0.05} when a polar solvent is used, a dual emission spectrum is observed in very dilute solutions (see Figure 3), and thus, at least that emission should also be observed in the solid-state spectrum of PFS_{0.05}, whereas it is not. Instead, the observation of a resolved emission at low S content suggests the lack of dipole–dipole interactions with surrounding molecules necessary to stabilize the ICT state.

The possibility that the broad emission observed in solid thin films is due to a simple aggregation effect is also unlikely. First, the emission matches quite well the spectrum observed in dilute solutions (see Figure S6 in Supporting Information), and second, despite the fact that the possibility of aggregation is present in all the samples, only those with higher S content, FSF and PFS_{0.3}, show the unresolved emission in the solid state.

The observation of a structured emission at low contents of S moieties and a broad unresolved spectrum at higher S contents must have a more profound explanation. The trend observed is consistent with the hypothesis that the increase in S content stabilizes the ICT state (see Scheme 2), and gives rise to an emission with less contribution from the LE state, and thus more unresolved emission. In this way, increasing the S content is equivalent to increasing the polarity of the bulk polymer matrix, leading to a self-induced solvatochromic shift. It should also be noted that in the case of PFDBT_{0.3} copolymer with high content of DBT units (30 mol %), similar to its behavior in chloroform solution (Figure 2b), PF-like emission is observed confirming its LE nature, with no signature of ICT emission (Figure 6).

2.3.2. Solvatochromism in the Solid State. The hypothesis of self-induced solvatochromism can be further tested by using the small oligomers FSF and FDBTF. This latter oligomer is a parent compound of FSF that does not show ICT-state formation. In contrast to FSF, where the dipole moment in the ground state is $\mu_G = 5.7$ D and the charge transfer reaction increases that value in the excited state, the ground-state dipole moment of FDBTF is small ($\mu_G = 1.4$ D) and no appreciable solvatochromism has been observed either in solution or in the solid

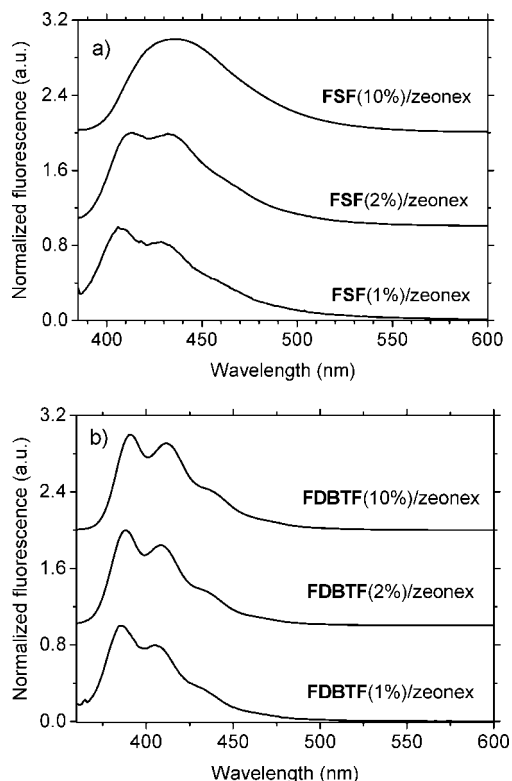


Figure 7. Normalized fluorescence spectra of (a) FSF and (b) FDBTF dispersed in a Zeonex matrix with three different co-oligomer/Zeonex ratios: 0.01, 0.02, and 0.1. Excitation wavelength at 390 nm.

state (Figure 7 and Figure S2 in Supporting Information). This strongly suggests that, once more, the observed broadening of the emission spectra is not a simple consequence of the concentration increase but rather an effect of self-induced ICT stabilization.

Figure 7 shows the emission spectra of FSF and FDBTF both dispersed in a Zeonex matrix with three different co-oligomer/Zeonex ratios: 0.01, 0.02, and 0.1. In these diluted solid-state solutions, Zeonex forms a nonpolar matrix and stabilization of the ICT state through motion of oligomers torsions is not possible. However, increasing the percentage of FSF affects the bulk polarity of the matrix, and thus a change in the emission profile of FSF is observed (Figure 7a). Clearly, the trend observed on going from low to high FSF content is that the emission shifts to longer wavelengths and becomes broader by analogy with the trend in solution, when increasing solvent polarity stabilizes the ICT state. Importantly, this effect is not observed in the case of FDBTF dispersed in Zeonex matrix where no ICT state is formed (Figure 7b).

2.3.3. Temperature Effect on the Emission Spectra. Figure 8 represents the temperature dependence of the emission spectra of PFS_{0.3} and PFDBT_{0.3} solid thin films. The emission spectrum of PFS_{0.3} appears broadened at 295 K, and with decreasing temperature a marked increase, up to 100%, in the integral fluorescence signal is observed (see inset in Figure 8b). Accompanying the increasing emission intensity, an increase in the degree of vibrational resolution with an isoemissive point around 450 nm is also observed. In contrast to that, only a small increase in the integral emission intensity of PFDBT_{0.3} is observed between 295 and 130 K (inset in Figure 8b), and with decreasing temperature the spectra become narrower and the intensity ratio between the first and second vibrational peaks, located at 430 and 456 nm, respectively, increases, indicating a restricted relaxation between the ground and excited states.

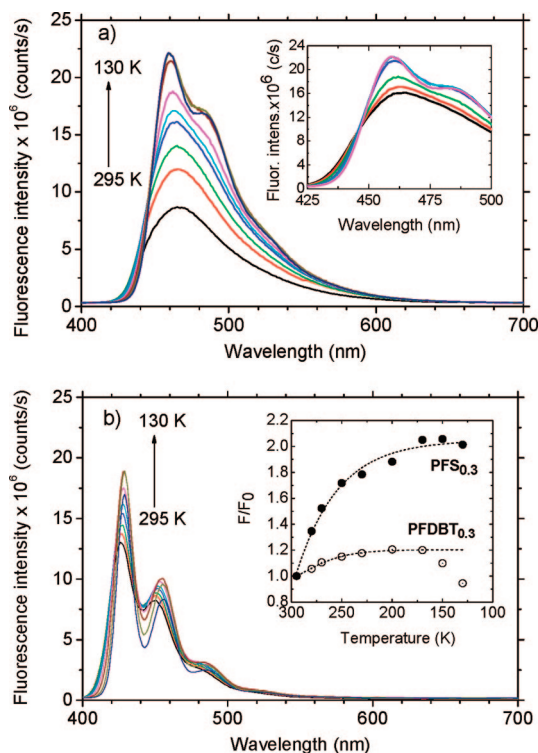


Figure 8. Fluorescence spectra of solid thin films, collected as a function of temperature between 295 and 130 K with excitation at 385 nm. (a) PFS_{0.3}; the inset shows a zoom of the main figure to highlight the isoemissive point observed between 250 and 130 K. (b) PFDBT_{0.3}; the inset shows the relative change in the integral of the emission spectrum of both compounds as a function of temperature. Arrows show decrease of the temperature.

The behavior found for PFDBT_{0.3} has previously been observed for other conjugated polymers and interpreted as a decrease in the Huang–Rhys parameter, as a result of increasing the conjugation length and exciton delocalization along the polymer chain with decreasing temperature, due to freezing of structural torsions and low-frequency vibrational modes that distort the polymer chain, making it more planar.¹⁷

The temperature dependence of PFS_{0.3} emission is consistent with the interpretation that the ICT state is stabilized by dipole–dipole interactions between the emission center and surrounding molecules. The tendency to planarity with decreasing temperature, observed in PFDBT_{0.3}, is counterbalanced by the reorientation of the bulk polymer molecules at the location of the excited solute, in order to stabilize the ICT state by dipole–dipole interactions. As a result, the emission spectrum of PFS_{0.3} is strongly affected by inhomogeneous broadening showing low vibrational resolution even at low temperatures.

2.3.4. Time Resolved Photoluminescence from Solid Thin Films. The hypothesis that the solvatochromism observed in the emission spectra of FSF and PFS_{0.3} films is the result of inhomogeneous broadening due to dipole–dipole interactions between the excited chromophore and surrounding molecules, leading to the ICT-state stabilization, can be further tested by the time resolved emission spectra of these two compounds. If such interactions are occurring, the emission decays and time resolved emission spectra (TRES) of FSF and PFS_{0.3} films should reflect it, by giving clear evidence of fast spectral dynamics.⁸ Furthermore, such effects should be absent in films of the model compounds, FDBTF and PFDBT_{0.3}, where the ICT state is not present and so no relaxation should occur.

Here the co-oligomer FSF represents a very useful model, because energy migration does not occur in this system;

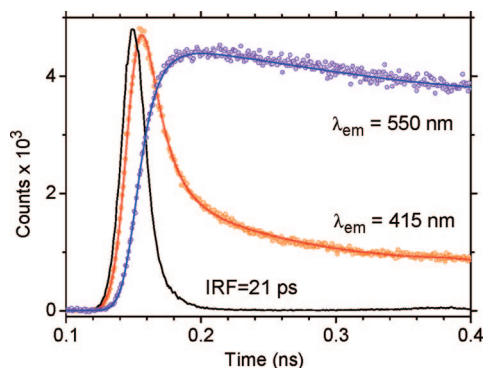


Figure 9. FSF time resolved fluorescence decays of FSF(10%)/Zeonex spin-coated on a quartz disk with emission collected at 415 and 550 nm. Note the sharp decay of the emission at 415 nm followed by a build in at 550 nm (see Table 2 for decay components and χ^2 values).

TABLE 2: Values of τ_i , A_i , and χ^2 from Global Analysis of Time Resolved Fluorescence Decays of FSF Thin Film at 293 K

λ_{em} (nm)	τ_4 (ns):[A_4]	τ_3 (ns):[A_3]	τ_2 (ns):[A_2]	τ_1 (ns):[A_1]	χ^2
400	0.009:[0.82]	0.085:[0.1]	0.606:[0.07]	2.57:[0.01]	1.06
550	0.009:[-0.27]		0.606:[0.46]	2.57:[0.54]	1.08

excitation populates the trimer but no longer conjugation segments are present in FSF. Figure 9 shows the time resolved fluorescence decay of FSF emission in a spin-coated film collected at 415 and 550 nm, respectively, on the blue and red sides of the emission spectrum. Global analysis of both decays (i.e., both decays were analyzed with common decay components) returns excellent fits when using sums of four and three discrete exponentials, respectively, for emission collected at 415 and 550 nm (Table 2).

The multiexponential nature of the decays is not surprisingly due to the heterogeneity of the solute surroundings and/or the nonexponential behavior of the relaxation processes involved; thus, no definitive physical meaning should be attributed to the decay components. However, for two of these decay times a clear interpretation is still possible (see Table 2 for details). The slower component with 2.57 ns is closely related to the ICT-state lifetime observed in ethanol solution, and the fast component around 9 ps, appearing markedly as a decay component at 400 nm and as a build in at 550 nm, behaves in a similar manner to the fast decay component assigned to the relaxation observed in ethanol (~ 30 ps).⁸

To exclude any potential effect of an experimental artifact, the fluorescence decay of FSF dispersed with 1% w/w fraction in a Zeonex matrix was also collected (see Figure S7 in Supporting Information). For this sample, the low percentage of FSF makes the matrix a nonpolar environment and the ICT stabilization does not occur. Consequently, the spectral dynamics observed in Figure 9 for high contents of FSF (10% w/w) should be absent at its low content. The experiment confirms this observation, and no fast component is observed for 1% w/w FSF in a Zeonex matrix (Figure S7 in Supporting Information).

What is striking in Figure 9 is the clearly noticeable spectral dynamics. Despite the fact that the sample is in the solid state, the chromophores, the bulk matrix molecules at the location of the excited solute, and possibly the solute itself, are still free to reorient and rearrange themselves in order to stabilize the new excited-state charge distribution of the solute.

Returning to the polymers, Figure 10 (top) shows the time resolved emission spectra (TRES) and (bottom) the emission

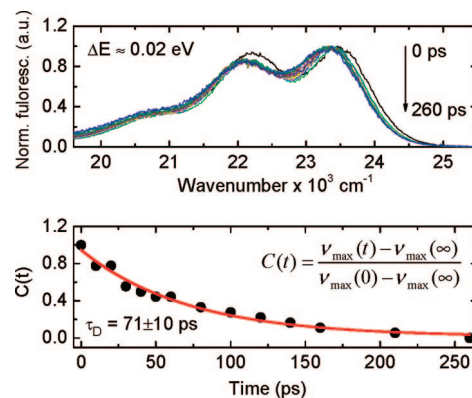


Figure 10. (top) Normalized time resolved emission spectra (TRES), and (bottom) emission energy correlation function $C(t)$ of PFDBT_{0.3} in a solid thin film. Excitation wavelength at 385 nm. The red line is a fit of $C(t)$ with single-exponential-decay function. Note the small stabilization energy (~ 0.02 eV) and the decay time constant of ~ 71 ps.

energy correlation function $C(t)$ of PFDBT_{0.3} in a solid film. The latter, in direct analogy to the correlation function used to study the solvation of polar fluorescent probes in polar liquids,¹⁸ is used to describe the spectral dynamics in a normalized scale, and in the case of conjugated polymers would reflect the influence of spectral relaxation processes as the excitation energy migration (EET) along the density of states (DOS), or the influence of molecular fluctuations in the vicinity of the excited solute that affects the emitting sites. The definition of $C(t)$ is given in Figure 10, with the spectrum recorded at 260 ps used to define the $\nu_{max}(\infty)$ value, since the spectral relaxation is completed by that time.

The spectral dynamics of PFDBT_{0.3}, showing a limited spectral relaxation of ~ 0.02 eV (on the order of KT at room temperature) and $C(t)$ decaying with 71 ps time constant, are clearly compatible with an isoenergetic EET process as a result of thermal fluctuations.¹³ EET in conjugated polymers is usually described as showing two different time regimes: i.e., one fast regime, occurring during the first few picoseconds or even on a subpicosecond time scale is referred to as dispersive or downhill EET, and another slower one, referred to as isoenergetic EET, can be observed over hundreds of picoseconds. Besides the time scale, both processes show different spectral signatures: while downhill EET gives a pronounced spectral shift, the isoenergetic counterpart occurs between states of similar energy and no significant spectral migration is observed.¹³

Figure 11 shows the TRES and the emission energy correlation function $C(t)$ of PFS_{0.3} in a solid thin film. The spectral relaxation observed in the case of PFS_{0.3} is clearly more pronounced than that for PFDBT_{0.3}. First, the spectral shift results in 0.12 eV stabilization, significantly larger than the KT value, which cannot be explained by only the rearrangement of the energetic polymer sites as a result of thermal fluctuations. Second, the emission energy correlation function in the case of PFS_{0.3} decays over a considerably longer time (~ 164 ps) than that observed for the PFDBT_{0.3}.

To understand the spectral dynamics present in solid films of PFS_{0.3}, we need to address first the role of energy migration in the population of FSF moieties in the copolymer chain. First, note that in the dilute solution the origin of the spectral dynamics is mainly intramolecular and PF-like emission is not observed even at short times. Second, intermolecular interactions in solid films tend to speed up excitation mobility due to a close

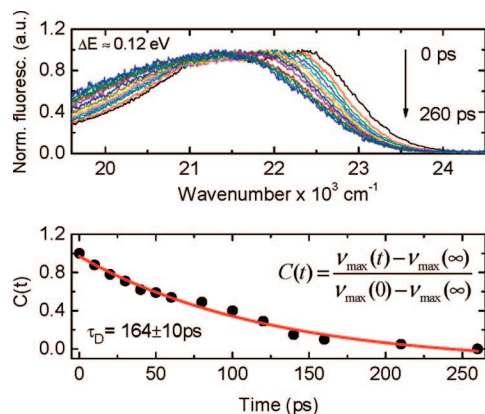


Figure 11. (top) Normalized time resolved emission spectra (TRES), and (bottom) emission energy correlation function $C(t)$ of PFS_{0.3} in a solid thin film. Excitation wavelength at 385 nm. The red line is a fit of $C(t)$ with a single-exponential-decay function. Note the pronounced spectral relaxation observed in the case of PFS_{0.3} (~0.12 eV) when compared with the almost relaxation free PFDBT_{0.3}, and the significantly longer (~164 ps) decay time of the correlation function.

proximity of neighboring chains that facilitate interchain hopping. Therefore, the absence in solution of PF-like emission, even at very short times, strongly suggests that any downhill energy migration in the solid state is below our time resolution; otherwise, PF-like emission would be observed in the most favorable case.

Furthermore, as mentioned above, the EET in conjugated polymers usually shows two different time scales, i.e., the dispersive regime occurring in a few picoseconds at most and giving rise to a strong spectral migration, and the isoenergetic regime which has little effect on the spectral diffusion. Clearly the behavior observed in the case of PFS_{0.3} is not compatible with this picture: the $C(t)$ decay is too long for a downhill process, and both the spectral dynamics and the energy stabilization value (0.12 eV) are not compatible with an isoenergetic EET scenario.

The spectral dynamics observed in solid films of PFS_{0.3} are, therefore, assigned to the stabilization of the ICT state due to the reorientation of the bulk polymer molecules at the location of the excited solute.

At variance to the behavior observed in chloroform solution, the emission spectrum of PFS_{0.3} in amorphous solid film appears initially structured with the vibrational features characteristic of the LE state, and progressively becomes broader, structureless, and red-shifted, showing at later times only the emission characteristic of the ICT state. In the solid state, the reorientation of the bulk polymer molecules in the vicinity of the excited solute, necessary to stabilize the excited-state charge distribution of the S-rich regions, progress at a slower rate than in solution. The radiative decay of PF-like emission is then able to compete with the ICT stabilization, and leads to the observation of PF-like emission at early times.

3. Experimental Section

3.1. Apparatus and Instrumentation. Absorption spectra were obtained using a Perkin-Elmer Lambda 19 double beam spectrophotometer in 1 cm path length quartz cells. Steady-state photoluminescence spectra were recorded on a Fluorolog (Jobin Yvon) fluorescence spectrometer with double excitation and emission monochromators using a right-angle configuration. Time resolved fluorescence decays were collected using the picosecond time correlated single photon counting technique (impulse response function, IRF = 21 ps). The excitation source,

with vertical polarization, was a picosecond Ti:sapphire laser from Coherent Inc. (wavelength range 720–1000 nm, 76 MHz repetition rate) coupled to a second-harmonic generator (360–500 nm). Emission collected at magic angle polarization was detected through a double subtractive monochromator, SpectraPro-2300i (Acton Research Corporation), by a Hamamatsu microchannel plate (MCPT), Model R3809U-50. Signal acquisition was performed using a TCSPC module from Becker & Hickl (Model SPC-630) using 4096 channels in a 0.8 ps/channel time scale. Deconvolution of the fluorescence decays was performed using the Globals WE software package.¹⁹ Random flat residuals between [−2,2] were obtained in all cases with χ^2 values close to unity. Time resolved spectra were acquired using a streak camera, Model C5680, from Hamamatsu, having 10 ps IRF.

Work performed in solution was carried out using dilute solutions with optical density below 0.2 at the maximum absorption wavelength, corresponding to concentrations of ~10^{−6} mol L^{−1}. The solvents with super purity grade were purchased from ROMIL and used as supplied. Amorphous solid thin films of all co-oligomers and copolymers were spin-coated from toluene solution with concentrations around 10 mg/mL.

3.2. Chemicals. The synthesis of co-oligomers FSF and FFSFF have been described previously.⁷ The copolymers PFS_x [$x = 0.02, 0.05, 0.15$ and 0.3 , and corresponds to molar fraction of S units in a random (9,9-dioctylfluorene)–(dibenzothiophene-*S,S*-dioxide) copolymer] used in this study had $M_w \sim 20\,000$ – $33\,000$ Da and $M_w/M_n \sim 1.5$. Their syntheses will be published elsewhere.⁹

3.2.1. 3,7-Dibromodibenzothiophene (2). 3,7-Dibromodibenzothiophene-*S,S*-dioxide (**1**)⁷ (4.00 g, 10.7 mmol) was suspended in dry diethyl ether (80 mL). LiAlH₄ (2.00 g, 52.7 mmol) was added slowly in portions with stirring to maintain a moderate reflux. When LiAlH₄ was added, the mixture was stirred at reflux for 6 h. Water was added dropwise (*carefully*!) to destroy excess LiAlH₄, and then the solution was diluted with water (~150 mL), heated with stirring to evaporate diethyl ether, and acidified with concentrated HCl (10 mL). The colorless solid was collected by filtration and washed with water. It was suspended again in a solution of concentrated HCl (20 mL) and water (300 mL), stirred for 20 min, filtered off, washed with water, and dried to afford crude product (3.20 g, 87%). The crude product was dissolved in chloroform (75 mL), filtered off from insoluble impurities, concentrated to ~25 mL, and left to crystallize, to yield compound **2** as colorless needles (1.63 g, 45%), mp 177.5–179.5 °C (lit.¹⁰ mp 169–170 °C). ¹H NMR (400 MHz, CDCl₃): $\delta = 7.98$ (2H, d, $J = 1.8$ Hz, H-4,6), 7.96 (2H, d, $J = 8.4$ Hz, H-1,9), 7.57 (2H, dd, $J = 1.8$ and 8.4 Hz, H-2,8). ¹³C NMR (100 MHz, CDCl₃): $\delta = 140.84, 133.65, 128.12, 125.43, 122.61, 120.76$. MS (EI): $m/z = 340$ (⁷⁹Br, ⁷⁹Br[M⁺], 52%), 342 (⁷⁹Br, ⁸¹Br[M⁺], 100%), 344 (⁸¹Br, ⁸¹Br[M⁺], 49%).

3.2.2. 3,7-Bis(9,9-di-*n*-hexylfluorene-2-yl)-dibenzothiophene (FDBTF). Under argon, to a mixture of 3,7-dibromodibenzothiophene (**2**) (1.00 g, 2.92 mmol), 9,9-di-*n*-hexylfluorene-2-boronic acid (**3**)⁷ (2.26 g, 5.97 mmol), and Pd(Ph₃P)₂Cl₂ catalyst (35 mg, 0.05 mmol), degassed 2.0 M potassium carbonate aqueous solution (12 mL) and 1,4-dioxane (20 mL) were added via syringe. The reaction mixture was stirred at 110 °C (oil bath) under argon for 21 h with protection from sunlight. The water layer was separated, and the organic layer was concentrated on a rotavapor (40 °C) and diluted with water, and a light brown solid was filtered off, washed with water, and dried. The crude product was purified by column chromatography on silica, eluted with a mixture of petroleum ether and dichloromethane (2:1 v/v) to obtain FDBTF (2.41 g, 97%)

as a yellowish powder. ^1H NMR (300 MHz, CDCl_3): δ = 8.26 (2H, d, J = 8.1 Hz, H-1,9 in DBT moiety), 8.16 (2H, d, J = 1.5 Hz, H-4,6 in DBT moiety), 7.82–7.65 (10H, m), 7.40–7.31 (6H, m), 2.07–2.01 (8H, m, $\text{CH}_2\text{C}_5\text{H}_{11}$), 1.18–1.00 (24H, m, $\text{CH}_2\text{CH}_2(\text{CH}_2)_3\text{CH}_3$), 0.77 (12H, t, J = 6.8 Hz, CH_3), 0.75–0.65 (8H, m, $\text{CH}_2\text{CH}_2\text{C}_4\text{H}_9$). ^{13}C NMR (100 MHz, CDCl_3): δ = 151.59, 151.03, 140.73, 140.70, 140.55, 140.51, 139.63, 134.33, 127.14, 126.83, 126.22, 124.15, 122.93, 121.77, 121.65, 121.19, 120.05, 119.81, 55.24, 40.46, 31.50, 29.73, 23.80, 22.58, 13.99. MS (EI+): m/z = 848.2 (M^+ , 100%). Anal. Calcd for $\text{C}_{62}\text{H}_{72}\text{S}$ (MW 849.30): C, 87.68; H, 8.54; S, 3.78. Found: C, 87.55; H, 8.50; S, 3.88.

3.2.3. Diocetylfluorene–Dibenzothiophene Copolymer PFDBT_{0.3}. Under argon, 3,7-dibromodibenzothiophene (**2**) (0.13 g, 0.38 mmol), 2,7-dibromo-9,9-dioctylfluorene (**4**) (0.14 g, 0.25 mmol), 9,9-dioctylfluorene-2,7-diboronic acid bis(1,3-propanediol) ester (**5**) (0.35 g, 0.63 mmol), $\text{Pd}(\text{Ph}_3\text{P})_4$ catalyst, and Aliquat 366 (0.4 mL) were added to a flask. To this mixture, a degassed solution of 2.5 M K_2CO_3 (1.6 mL, 4 mmol) and a degassed mixture of toluene:dioxane (3:1, v/v; 6 mL) were added via syringe and the reaction mixture was stirred at 110 °C for 80 h. For end-capping of the polymer, 0.42 M solution of 4-*n*-butylbromobenzene in toluene (0.2 mL) was added and the mixture was stirred at 110 °C for 12 h. Then 0.34 M solution of 4-*n*-butylbenzeneboronic acid (0.2 mL) was added and the mixture was stirred at 110 °C for an additional 12 h. After cooling, the mixture was poured into warm methanol (80 mL) with vigorous stirring, concentrated HCl (20 mL) was added, and the solid was filtered off, washed with methanol:acetone, 1:1 v/v (20 mL), methanol:acetone:water, 1:1:1 v/v/v (20 mL), methanol:acetone, 1:1 v/v (10 mL), and dried. The resulting greenish-yellow solid was placed in a thimble and extracted in a Soxhlet apparatus with acetone for 20 h. After removal of the acetone from the thimble under vacuum, the residue was extracted into chloroform. The chloroform solution was concentrated under reduced pressure to ~5 mL and poured dropwise into warm methanol (100 mL) with vigorous stirring. Acetone (10 mL) and concentrated HCl (3 mL) were added to this mixture with stirring and the fibrous precipitate was filtered, washed with methanol:acetone, 1:1 v/v, and dried in vacuo at room temperature to afford copolymer PFDBT_{0.3} (0.36 g, 88%). Size exclusion chromatography (SEC, vs polystyrene standard): M_w = 56 500 Da, M_n = 23 200 Da, PDI = 2.44. Thermal decomposition: $T_d^{5\%}$ = 397 °C.

4. Conclusion

In agreement with previous findings for FSF co-oligomers,⁸ the excited-state dynamics of PFS_x copolymers are dominated by an intramolecular excited-state charge transfer state which is stabilized, both in solution and in the solid state, by dipole–dipole interactions with the surrounding medium. In the solid state, the effect of the environment on the stabilization of the ICT state progresses at a slower rate than in solution, giving rise to a solvatochromic effect with the emission peaking at around 440 nm with clearly defined vibronic replicas at low S content, changing to structureless and red-shifted emission around 470 nm at higher S content. The temperature dependence of the emission spectra of $\text{PFS}_{0.3}$ and PFDBT_{0.3} in the solid state shows that negating the stabilization of the ICT state strongly increases the fluorescence quantum efficiency in the solid state. These results provide new insights into processes involved in emission from conjugated copolymers. The ap-

plicability of these copolymers as PLED materials will be reported in due course.

Acknowledgment. The authors thank the DTI and Thorn Lighting for funding this work via the “Thin Organic Photoconductive Light-Emitting Surfaces” (“TOPLESS”) project. I.I.P. and M.A.K. thank M.R.B. for the opportunity to visit Durham University.

Supporting Information Available: Absorption and emission spectra; time resolved fluorescence decays. This material is available free of charge via the Internet at <http://pubs.acs.org>.

References and Notes

- (1) Burroughes, J. H.; Bradley, D. D. C.; Brown, A. R.; Marks, R. N.; Mackay, K.; Friend, R. H.; Burn, P. L.; Holmes, A. B. *Nature* **1990**, *347*, 539–541.
- (2) *Handbook of Conducting Polymers. Conjugated Polymers*, 3rd ed.; Skotheim, T. A.; Reynolds, J. R., Eds.; CRC Press: Boca Raton, FL, 2007; Vols. 1 and 2.
- (3) Perepichka, D. F.; Perepichka, I. F.; Meng, H.; Wudl, F. Light-Emitting Polymers. In *Organic Light-Emitting Materials and Devices*; Li, Z.; Meng, H., Eds.; CRC Press: Boca Raton, FL, 2007; Chapter 2, pp 45–293.
- (4) (a) Friend, R. H.; Gymer, R. W.; Holmes, A. B.; Burroughes, J. H.; Marks, R. N.; Taliani, C.; Bradley, D. D. C.; Dos Santos, D. A.; Brédas, J. L.; Lögdlund, M.; Salaneck, W. R. *Nature* **1999**, *397*, 121–128. (b) McGehee, M. D.; Heeger, A. J. *Adv. Mater.* **2000**, *12*, 1655–1668. (c) Bernius, M. T.; Inbasekaran, M.; O'Brien, J.; Wu, W. *Adv. Mater.* **2000**, *12*, 1737–1750. (d) Akcelrud, L. *Prog. Polym. Sci.* **2003**, *28*, 875–962. (e) Forrest, S. R. *Nature* **2004**, *428*, 911–918. (f) Babudri, F.; Farinola, G. M.; Naso, F. *J. Mater. Chem.* **2004**, *11*, 11–34. (g) Perepichka, I. F.; Perepichka, D. F.; Meng, H.; Wudl, F. *Adv. Mater.* **2005**, *17*, 2281–2305. (h) Muccini, M. *Nat. Mater.* **2006**, *5*, 605–613.
- (5) (a) Scherf, U.; List, E. J. W. *Adv. Mater.* **2002**, *7*, 477–487. (b) Neher, D. *Macromol. Rapid Commun.* **2001**, *22*, 1366–1385.
- (6) (a) Kraft, A.; Grimsdale, A. C.; Holmes, A. B. *Angew. Chem., Int. Ed.* **1998**, *37*, 402–428. (b) Mitschke, U.; Bauerle, P. *J. Mater. Chem.* **2000**, *10*, 1471–1507.
- (7) Perepichka, I. I.; Perepichka, I. F.; Bryce, M. R.; Pålsson, L.-O. *Chem. Commun.* **2005**, 3397–3399.
- (8) Dias, F. B.; Pollock, S.; Hedley, G.; Pålsson, L.-O.; Monkman, A.; Perepichka, I. I.; Perepichka, I. F.; Tavasli, M.; Bryce, M. R. *J. Phys. Chem. B* **2006**, *110*, 19329–19339.
- (9) King, S. M.; Perepichka, I. I.; Perepichka, I. F.; Dias, F. B.; Bryce, M. R.; Monkman, A. P. To be submitted.
- (10) Sirringhaus, H.; Friend, R. H.; Wang, C.; Leuninger, J.; Müllen, K. *J. Mater. Chem.* **1999**, *9*, 2095–2101.
- (11) Terenziani, F.; Painelli, A.; Katan, C.; Charlot, M.; Blanchard-Desce, M. *J. Am. Chem. Soc.* **2006**, *128*, 15742–15755.
- (12) Grabowski, Z. R.; Rotkiewicz, K.; Rettig, W. *Chem. Rev.* **2003**, *103*, 3899–4031.
- (13) Scheblykin, I. G.; Yartsev, A.; Pullerits, T.; Gulbinas, V.; Sundstrom, V. *J. Phys. Chem. B* **2007**, *111*, 6303–6321.
- (14) (a) Dias, F. B.; Knaapila, M.; Burrows, H.; Monkman, A. *Macromolecules* **2006**, *39*, 1598–1606. (b) Dias, F. B.; Maiti, M.; Hintschich, S. I.; Monkman, A. P. *J. Chem. Phys.* **2005**, *122*, 054904. (c) Dias, F. B.; Morgado, J.; Maçanita, A. L.; Costa, F. P.; Burrows, H.; Monkman, A. *Macromolecules* **2006**, *39*, 5854–5864. (d) Dias, F. B.; Maçanita, A. L.; Seixas de Melo, J. S.; Burrows, H.; Guntner, R.; Scherf, U.; Monkman, A. P. *J. Chem. Phys.* **2003**, *118*, 7119–7126.
- (15) Anémian, R.; Mulatier, J.-C.; Andraud, C.; Stéphan, O.; Vial, J.-C. *Chem. Commun.* **2002**, 1608–1609.
- (16) (a) Hintschich, S. I.; Dias, F. B.; Monkman, A. P. *Phys. Rev. B* **2006**, *74*, 45210–45219. (b) Movaghar, B.; Grunewald, B.; Ries, B.; Bassler, H.; Wurtz, D. *Phys. Rev. B* **1986**, *33*, 5545–5554. (c) Franco, I.; Tretiak, S. *J. Am. Chem. Soc.* **2004**, *126*, 12130–12140.
- (17) (a) Lim, S.; Bjorklund, G.; Bardeen, C. J. *Chem. Phys. Lett.* **2001**, *342*, 555–562. (b) Guha, S.; Rice, J. D.; Yau, Y. T.; Martin, C. M.; Chandrasekhar, M.; Chandrasekhar, H. R.; Guentner, R.; Scanducci de Freitas, P.; Sherf, U. *Phys. Rev. B* **2003**, *67*, 125204–125209.
- (18) (a) *Principles of Fluorescence Spectroscopy*, 2nd ed.; Lakowicz, J. R., Ed.; Kluwer Academic/Plenum Publishers: New York, 1999; p 220. (b) Pal, S. K.; Peon, J.; Zewail, A. H. *Proc. Natl. Acad. Sci. U.S.A.* **2002**, *99*, 1763–1768.
- (19) Beechem, J. M.; Gratton, E. *Proc. SPIE* **1988**, *909*, 70–81.